

STUDY ON NOISE OF COUNTER ROTATING FAN MODELS AT CIAM ANECHOIC CHAMBER

Yuri Khaletskiy*, Victor Mileschin, Jerome Talbotec***, Eberhard Nicke******

*** ** CIAM, 2, Aviamotornaya str. 111116, Moscow, Russia**

***** Snecma groupe Safran, France**

****** German Aerospace Center (DLR), Germany**

yurikhalet@ciam.ru; mileschin@ciam.ru; jerome.talbotec@snecma.fr, eberhard.nicke@dlr.de

Keywords: *noise, counter rotating fan, combination frequency*

Abstract

Nowadays searching of new engine designs providing advanced efficiency is priority task of leading aero engine companies. It is supposed, that such new schemes should provide further noise abatement, engine weight decrease, reliability, efficiency and stall margin increase. Achievements in bypass engine design methods have called revival of interest to ducted counter rotating fans. Consequence of this was creation in CIAM facility for testing counter rotating fan models in the anechoic chamber.

Ducted counter rotating fan reaches bypass ratio equal to 10...15 and thereby provides fuel consumption benefit 15...20%. Achievement can be linked also with the progress in techniques of blade rows manufacturing and also with the lightweight blades made of composite materials.

Under VITAL Project funded by the European Community, Snecma as a project leader developed a counter rotating low-speed fan concept for a high bypass ratio engine [1-5].

Results of experimental studying of three counter rotating fan models of 22 inches diameter at CIAM anechoic chamber were considered. CRTF1 fan model blades were manufactured from thin solid titanium. Profile of CRTF2a fan model blades simulates blades made of composite material. Carbon-filled plastic blade in comparison with the solid titanium blade has essentially thicker edges and bigger maximum thickness. Third counter rotating fan model CRTF2b has been manufactured according to «Blisk» technology.

Availability at noise spectra a lot of number of discrete noise components at BPF1,

BPF2 and their harmonics and also components on their combinational frequencies is characteristic feature for all tested models. Discrete components of noise at combinational frequencies basically determine fan noise spectrum over working frequency range.

It is shown that CRTF2A fan model with thickened blades is noisier than CRTF1 fan model. Comparison of their spectra at the same modes reveals that at combinational frequencies occurs acoustic energy redistribution. Discrete component at summary frequency $BPF1 + BPF2$ dominates at noise spectrum of CRTF1 fan model and third harmonics at frequency $3*(BPF1+BPF2)$ dominates at noise spectrum of CRTF2a fan model. Thus broadband noise of CRTF2a fan model with thickened blades is on 3...5 dB higher than of CRTF1 fan model.

The third fan model CRTF2b was designed as an economic version with reduced blade numbers (minus 20 %) and reduced axial gap between both rotors. On one side an efficiency benefit of roughly 2%-points with the same or even better stall margin was reached. On the other side this version was significant noisier. This result was not unexpected as value of axial clearance between rotors almost is twice less, than at another tested two models.

Noise prediction with the most silent model CRTF1 equipped with sound absorbing liner has significant margin relative to ICAO Chapter 4.

1 Introduction

Nowadays searching of new engine designs providing advanced efficiency is

priority task of leading aero engine companies. It is supposed, that such new schemes should provide further noise abatement, engine weight decrease, reliability, efficiency and stall margin increase. The steady tendency in increasing the bypass ratio of turbofan engine leads to a fan tip speed reduction and eventually to a favourable effect on the noise performances of the whole engine. One trend in development of engine configuration with high bypass ratio is ducted counter rotating fan architecture. Such scheme gives us an opportunity to realize an engine configuration with the bypass ratio $m=25$ and fuel consumption reduction on 15...20%. Progress is also stipulated by development of new technologies in blade row manufacturing and the lightened blades production technology including composite blades.

Earlier in frame of CRISP program (Counter Rotating Integrated Shrouded Propfan) acoustic response of ducted counter rotating fans were studied [6, 7]. Ducted counter rotating fan models with diameter 320, 400 and 100 mm were manufactured and investigated according to CRISP program. But noise levels of these fan models proved to be essentially higher than expected.

In frame of European project VITAL (Environmentally Friendly Aero Engine) acoustic tests of three counter rotating fan models with pressure ratio 1.56 (CRTF1, CRTF2a), 1.5 (CRTF2b) and diameter, equal to 22 inches have been performed at the CIAM test facility. There were several main goals in this work: study of differences in noise spectrum of counter rotating and conventional single rotor fan models and comparison of noise spectrum of three counter rotating fan models, manufactured according to different technologies. So, CRTF1 mockup has thin titanium rotor blades, profile of CRTF2A model titanium thickened blades simulates the composite blades. The third counter rotating fan model differed in design by number of rotor blades and twice less axial gap between front and aft rotor.

2 Anechoic chamber of CIAM C-3A test facility for counter rotating fan models testing

The anechoic chamber of CIAM C-3A test rig is a square room of 1150 m³ volume and the following linear sizes: 5.0 m height, 15.6 m length and 14.7 m width. The chamber walls are covered by porous sound-absorbing material partially "vinipor" and partially "periotek" [8]. C-3A test facility acoustic data acquisition system includes 24 measuring channels, every one of which consists of 4939-type microphone (1/4 inches diameter), 2670-type preamplifier, AO 0416 cable (2×30 m length) and four-channel amplifier NEXSUS of 2690-type (all components are manufactured by B&K company). During experimental work all microphones are equipped by windshield screen of UA 0459 type by B&K Company.

Microphones were installed in directions from 10° up to 160° with the step 5 – 10° along two arcs with the radius, equal to 4.0 m relative to the leading edge of the front rotor and the nozzle section according to the scheme, represented at Fig. 1.

All measuring channels are connected to two multichannel recorder-analyzers MIC-300 by MERA Company, assembled on base of personal computer. Multichannel system of microphone signal recording and analysis is realized on base of PCI card 2428. Frequency operating range: 0 – 100 kHz.

The software allows providing 1/3-octave and narrow-band analysis (maximal number of lines - 8192). Also the software allows generating the output information in ASCII format. Hardware-analyzing complex is consistent with the ISO operating standards, applying to recording and analyzing acoustic equipment.

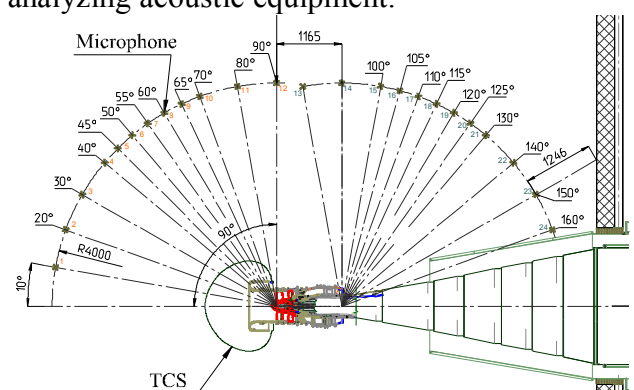


Fig. 1. Scheme of microphone location in the anechoic chamber of CIAM test rig

3 Results of counter rotating fan models noise investigation

3.1 Acoustic response of CRTF1 fan model

Let us consider acoustic response of CRTF1 fan mockup, obtained at 3 operating modes – Runway, Flyover and Approach. Characteristic feature of counter rotating fan acoustic response is noise generation at not only blade passing frequencies of its elements – R1, R2 and R3 (booster), but at multiplicity of combination frequencies initiated by interaction of these elements acoustic fields [9]. Let us designate blade passing frequencies of fan first and second rotor as f_1 and f_2 , and booster – f_3 . At this passing frequency is defined as $f = z N/60$ (Hz), where z – number of rotor blades, N – rotor rotational frequency, RPM.

In principle, acoustic field of such a system comprises of all the frequencies described by the formulation:

$$f = mf_1 + nf_2 + pf_3 \quad (1)$$

where m, n, p – random integers. However actually acoustic fields inside the fan channel at most frequencies are weak as waves at these frequencies attenuate exponentially and because of low level of their generation.

So rotor of internal duct (booster), located near the fan axis, has relatively low circumferential speed. As a result its noise level is significantly lower, than noise level of R1 and R2. Besides, R3 noise, before radiating into the environment, has to pass through the R1 (upstream) or change the direction and pass through the R2 (downstream). In both cases the noise will be additionally strongly weakened.

3.1.1 Runway

Fig. 2 represents direction-averaged narrowband spectra of counter rotating fan model at Runway mode.

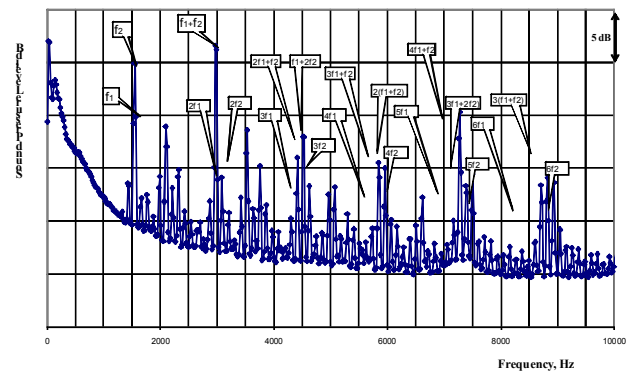


Fig. 2. Direction-averaged narrowband spectra of counter rotating fan model CRTF1 at Runway mode
It is seen that the tonal components are dominating at frequencies described as:

$$f = mf_1 + nf_2 \quad (2)$$

where $m > 0$ and $n > 0$.

It should be noted, that at Runway mode tones at BPF and its harmonics mf_1 and nf_2 ($m > 0$ and $n > 0$) proved to be relatively lower than components at combination frequencies $f = mf_1 + nf_2$ ($m > 0$ and $n > 0$).

Fig. 3 represents Runway narrowband spectra of counter rotating fan model for maximal radiation direction 120° in rear hemisphere (with and w/o hush kit installation).

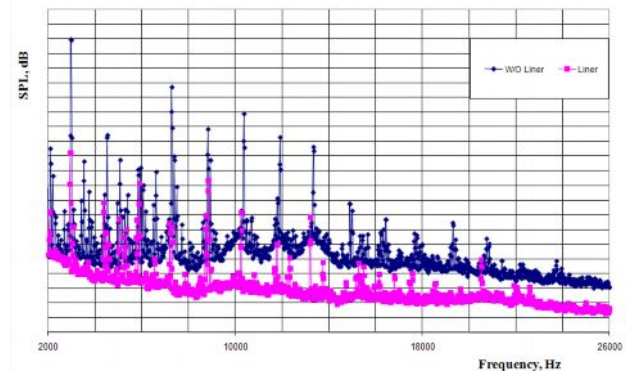


Fig. 3. Runway narrowband spectra of counter rotating fan model CRTF1 in direction 120°

It is seen that the tonal components were reduced more essentially in comparison with the broadband noise. Besides, the noise reduction increases as the noise radiation angle increases.

Fig. 4 represents noise directivity diagram regarding to fan mockup without hush kit installation for some of 1/3-octave frequencies. It is clearly seen that the noise is radiating mostly in rear hemisphere, so at Runway mode the fan is an unbalanced noise source.

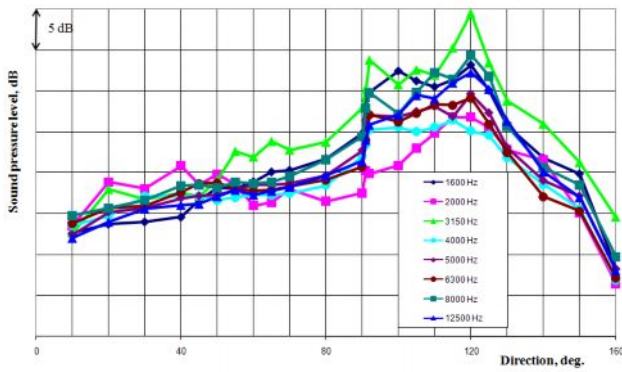


Fig. 4. Noise directivity diagram (w/o hush kit installation) at Runway

Fig. 5 represents noise directivity diagram regarding to fan mockup with hush kit installation. It is seen that homogeneous liner used in the fan duct are quite effective within the wide frequency range; at the same time reducing the noise more significantly in rear hemisphere. Noise reduction was equal to 15 dB in 1/3-octave frequency band with the band center frequency 3150 Hz in direction of noise radiation 120°. On the whole, at all frequencies higher than 5 kHz maximal noise absorption is observed exactly in rear hemisphere. In spite of this fact, noise radiation is dominating in rear hemisphere for fan mockup with hush kit installation, so at Runway mode the fan is still an unbalanced noise source.

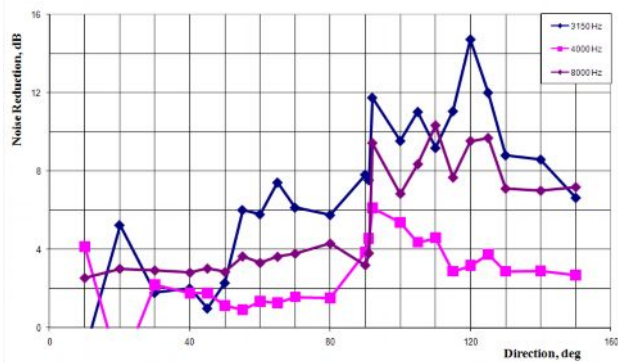


Fig. 5. Directivity diagram of noise reduction with hush kit installation at Runway

3.1.2 Flyover

Fig. 6 represents direction-averaged narrowband spectra of counter rotating fan model at Flyover mode.

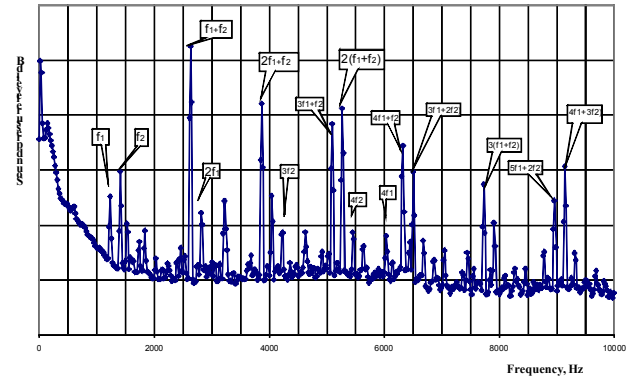


Fig. 6. Direction-averaged narrowband spectra of counter rotating fan model CRTF1 at Flyover mode (w/o hush kit installation)

It is seen that the tonal components are dominating at frequencies $f = mf_1 + nf_2$, where $m > 0$ and $n > 0$. Though components at frequencies $f = mf_1 + nf_2 + pf_3$, where $m > -2$, $n > 0$, $p = 1$, are appeared but have very low levels. The same way as for the Runway mode, tones at BPF of first and second Rotor and its harmonics mf_1 and nf_2 ($m > 0$ and $n > 0$) proved to be relatively lower than components at combination frequencies $f = mf_1 + nf_2$ ($m > 0$ and $n > 0$).

Fig. 7 represents noise directivity diagrams regarding to fan mockup without hush kit installation for some of 1/3-octave frequencies. It is also seen that the noise is radiating mostly in rear hemisphere, but to a less extent re the Runway mode.

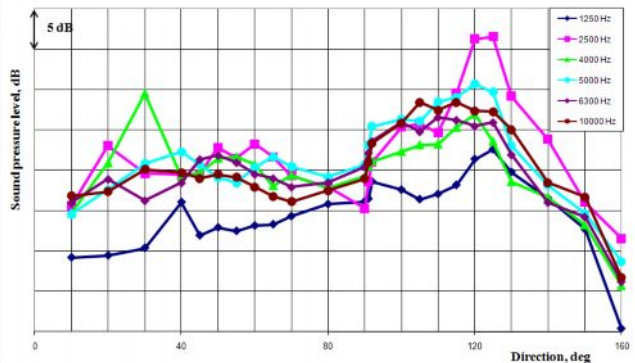


Fig. 7. Directivity diagram of noise reduction without hush kit installation at Flyover

Fig. 8 represents noise directivity diagram regarding to fan mockup with hush kit installation. It is seen that homogeneous liner used in the fan duct are quite effective within the wide frequency range; at the same time reducing the noise more smoothly in forward and rear hemispheres. Again, noise radiation is dominating in rear hemisphere for fan mockup

CRTF1 with hush kit installation, but to a less extent re the Runway mode.

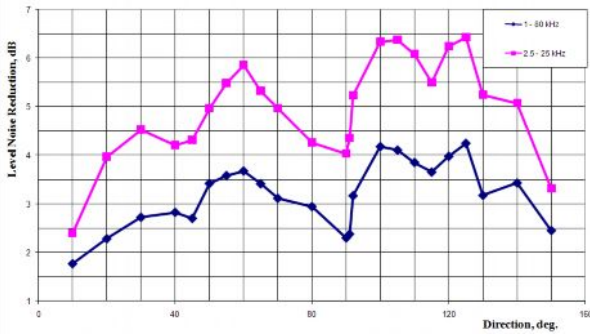


Fig. 8. Averaged directivity diagrams of noise reduction at hush kit installation at Flyover mode

3.1.3 Approach

Fig. 9 represents direction-averaged narrowband spectra of counter rotating fan model at Approach mode. It is seen that the tonal components are dominating at frequencies $f = mf_1 + nf_2$, where $m > 0$ and $n > 0$. Noise components at frequencies, closely related to booster presence, practically were not discovered.

Noise tones at BPF of R1 and R2 and its harmonics mf_1 and nf_2 ($m > 0$ and $n > 0$) proved to be relatively lower than components at combination frequencies $f = mf_1 + nf_2$ ($m > 0$ and $n > 0$).

As a result of hush kit installation, the tonal components were reduced more essentially in comparison with the broadband noise. But the broadband noise reduction appeared to be also quite significant – 6...8 dB.

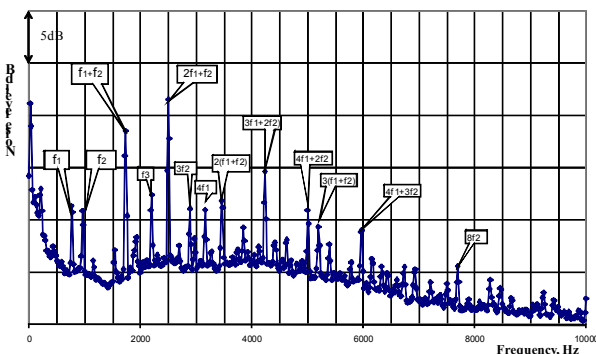


Fig. 9. Direction-averaged narrowband spectra of counter rotating fan model CRTF1 at Approach

Fig. 10 and 11 represent noise directivity diagram regarding to fan mockup with and without hush kit installation for some of 1/3-octave frequencies. It is clearly seen that with

and without hush kit installation the fan noise is practically close to the balanced one. In 1/3-octave frequency band with the band center frequency 2500 Hz, that is, at frequency $(2f_1 + f_2)$, radiation of noise in forward hemisphere exceeds its radiation in rear hemisphere.

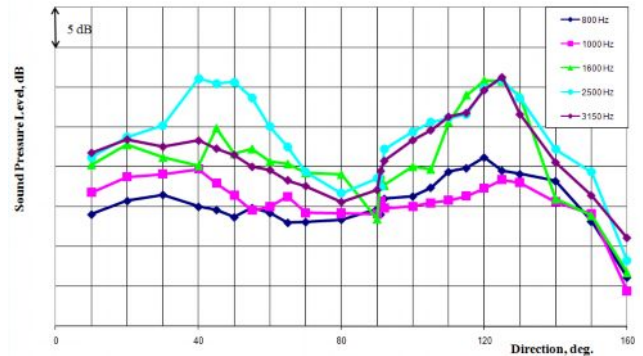


Fig. 10. Noise directivity diagram (w/o hush kit installation) at Approach

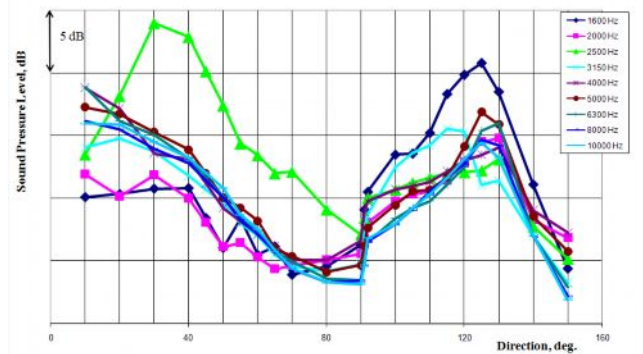


Fig. 11. Noise directivity diagram (with hush kit installation) at Approach

At last, Fig. 12 and 13 represent 1/3-octave spectra and directivity diagram of noise reduction regarding to fan mockup with hush kit installation. Again it is seen, that liners, used in the fan duct are quite effective within the wide frequency range; at the same time reducing the noise more smoothly in forward and rear hemispheres (Fig. 14).

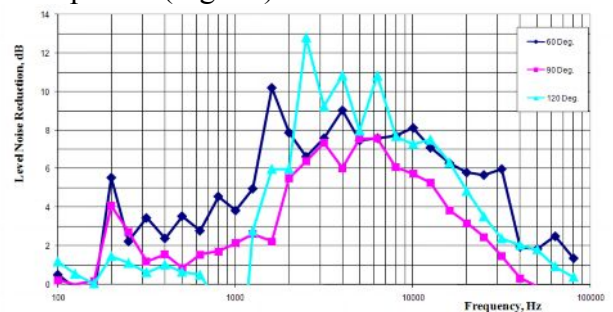


Fig. 12. 1/3-octave spectra of noise reduction with hush kit installation in different radiation angles at Approach

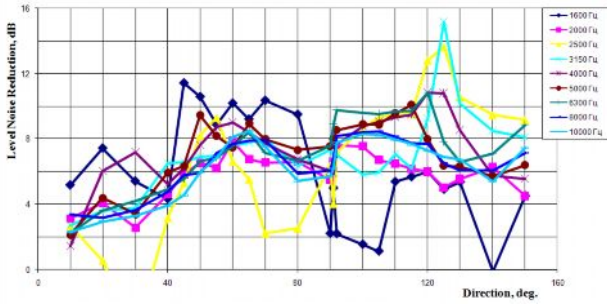


Fig. 13. Directivity diagram of noise reduction (with hush kit installation) at Approach

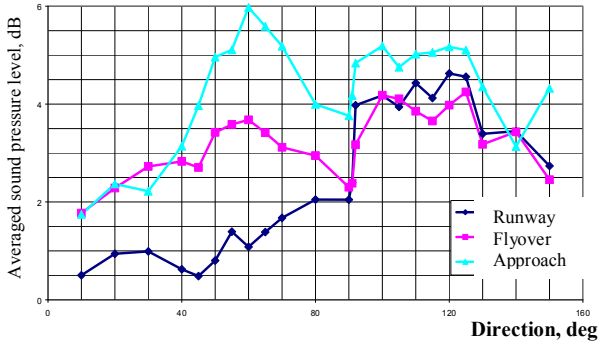


Fig. 14. Averaged by 1 - 80 kHz frequencies directivity diagram of noise reduction with hush kit installation

At the end of this chapter directivity diagrams of averaged noise are represented in Approach mode at frequencies f_1 , f_2 , (f_1+f_2) and $(2f_1+f_2)$ as a result of hush kit installation (Fig. 15). This plot draws attention to the following. Noise reduction at BPF of R1 and R2 is insignificant at frequencies f_1 and f_2 (Fig. 15); moreover, in rear hemisphere weak noise generation was observed after hush kit installation. So, frequencies f_1 and f_2 demonstrated the lower limit of the efficiency of the liners, used in the CRTF1 fan model duct. Concerning the influence of noise level on the noise reduction efficiency, it was obtained, that the noise reduction efficiency increased as a result of operating mode increasing.

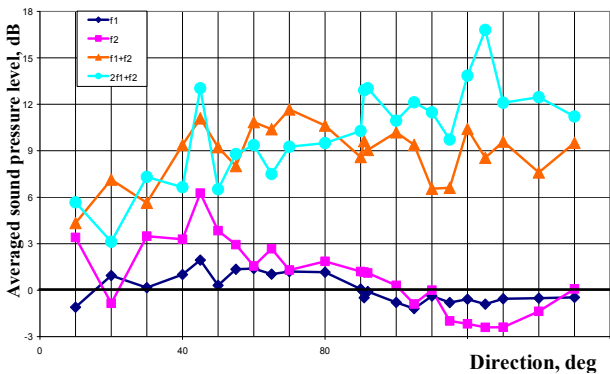
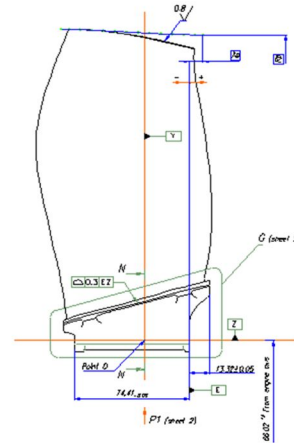


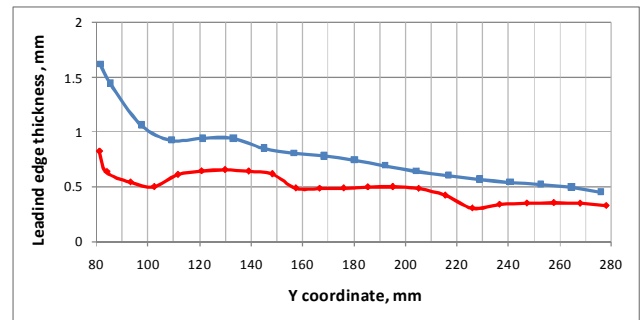
Fig. 15. Directivity diagrams of averaged noise reduction at frequencies f_1 , f_2 , f_1+f_2 and $2f_1+f_2$ in Approach as a result of hush kit installation

3.2 Influence of rotor blade shape on noise levels of counter rotating fan model

F1 mockup has conventional thin titanium rotor blades, profile of F2 model titanium blades simulates the composite blades with thickened edges (Fig. 16, 17). The lightened carbon plastic blade has thicker edges and maximal thickness relative to the solid titanium blade.



Issue of counter rotating fan blades thickness influence on noise generation is raised in connection with tendency of engine weight reduction by means of using blades of light composite materials. In particular CIAM developed light carbon-filled plastic blades technology [10]. In spite of the fact, that carbon-filled plastic blade is twice lighter than the solid blade of titanium the first one is thicker on 20-30% with noticeably thicker edges. It is clear that one of the mechanisms of fan broadband noise generation is interaction of vortexes descending from the blade trailing edge of the first rotor with the second rotor blades. Consequently broadband noise level depends on rotor blade thickness.



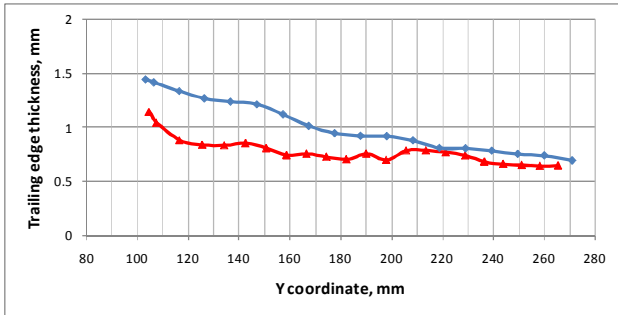


Fig. 17. Change in thickness of rotor blade leading and trailing edge along Y-coordinate
 — - CRTF1 model, — - CRTF2a model

Comparison of acoustic response of two counter rotating fan models: with titanium blades (F1 model) and with blades, profile of which simulated the composite blades (F2 model) showed the following.

CRTF2a counter rotating fan model with thickened blades generates noise, higher than of the CRTF1 model on 2...3 dB (Fig. 18). Components at frequency $3*(f_1 + f_2)$ and its harmonics dominate in CRTF2a model noise spectrum at forward hemisphere in Runway and Flyover conditions; while components at frequency, equal to the sum of R1 and R2 BPF, i.e. $(f_1 + f_2)$ dominate in CRTF1 model noise spectrum. At this difference in maximal level of spectra under study is 7 dB (Fig. 18), with benefit of CRTF2a model.

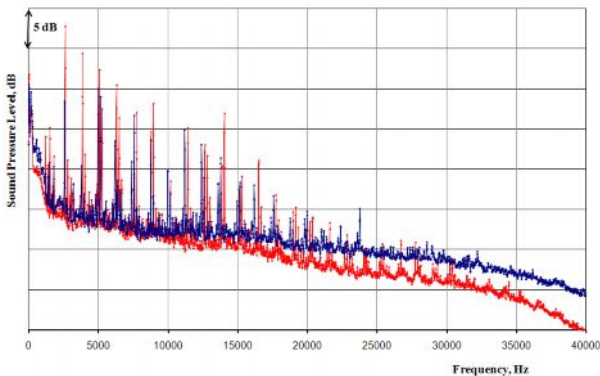


Fig. 18. Narrowband spectra of counter rotating fans – CRTF1 (red line) and CRTF2a model (blue line) at Flyover mode in direction 60°

Meanwhile correlation between tonal noise levels of two fan models is ambiguous. At Runway and Flyover modes in rear hemisphere tonal noise of CRTF1 model is higher than tonal noise of CRTF2a model (Fig. 19).

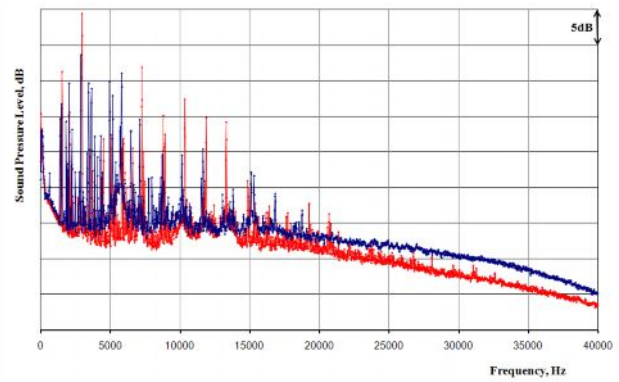


Fig. 19. Narrowband spectra of counter rotating fans – CRTF1 (red line) and CRTF2a model (blue line) at Runway mode in direction 120°

Predictions discovered that cumulative noise level of hypothetical aircraft, powered by engine with CRTF2a fan, is higher on 10 EPNdB than the same aircraft, powered by engine with CRTF1 fan.

Thus, test results of two counter rotating fan models showed, that counter rotating fan noise spectrum is characterized by availability of the number of tonal components as at R1 and R2 BPF and its harmonics as combination frequencies including these noise sources interactions. And just tonal components at combination frequencies determine fan noise level at operating frequency range.

It is shown that CRTF2a model with thickened blades generates noise of higher sound level than CRTF1 model.

3.3 Comparison of acoustic response of counter rotating fan models differ by number of rotor blades and axial gap value

Narrowband spectra of counter rotating fan model CRTF2b at Runway conditions, averaged in forward hemisphere direction 30°-60°, are represented in Fig. 20; and, averaged in rear hemisphere direction 110°-120°, are represented in Fig. 21. It is seen that in forward hemisphere tonal noise components at combination frequencies f_1+f_2 ; $2*f_1+f_2$; $3*f_1+f_2$ are the most power contributors to the cumulative fan noise.

The most power carrying component at frequency $2*f_1+f_2$ exceeds tonal components at R1 passing frequency on 14 dB, at R2 passing frequency - on 12 dB, that is these components of counter-rotating fan noise practically don't

contribute to the total noise level, in contrast to the one stage fan, in which tonal noise at passing frequency is dominant (Fig. 20). In rear hemisphere noise spectrum includes even more number of power carrying components. In addition to components at frequencies f_1+f_2 ; $2*f_1+f_2$; $3*f_1+f_2$, dominating in forward hemisphere, components at combination frequencies $2(2f_1+f_2)$; $3f_1+f_2$; $3(f_1+f_2)$; $3f_1+2f_2$ are added (Fig. 21).

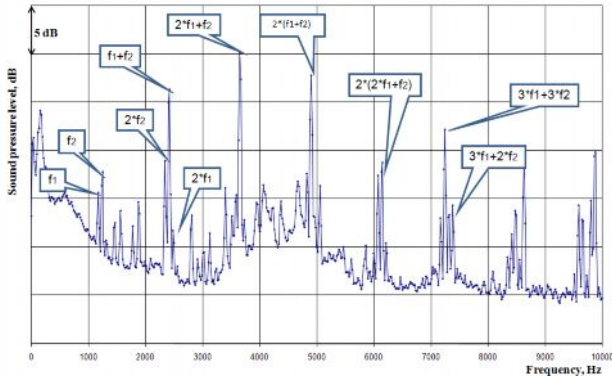


Fig. 20. Narrowband spectra of counter rotating fan model CRTF2b at Runway mode in direction 60°

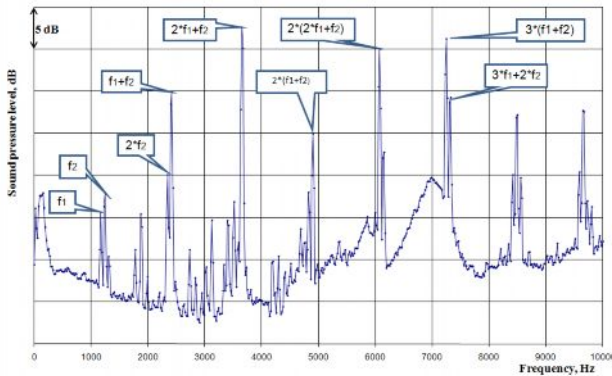


Fig. 21. Narrowband spectra of counter rotating fan model CRTF2b at Runway mode in direction 120°

Fig. 22 represents directivity diagrams of tonal noise components f_1 , f_2 ; f_1+f_2 ; $2*f_1+f_2$ of counter rotating fan model. It is clearly seen that at Runway mode the fan is an unbalanced noise source, as the noise, radiating in rear hemisphere, significantly exceeds the noise, radiating in forward hemisphere due to the flow convection.

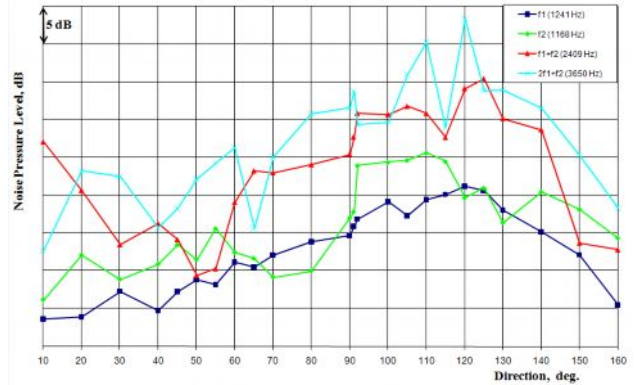


Fig. 22. Directivity diagrams of tonal noise components of counter rotating fan model CRTF2b at Runway mode. In contrast to the Runway conditions at Flyover conditions most power carrying components at R1 and R2 passing frequency and their harmonics mf_1 and nf_2 ($m > 0$ and $n > 0$) turned out to be higher in comparison with the components at combination frequencies $f = mf_1 + nf_2$ ($m > 0$ and $n > 0$). At this noise levels of harmonics with higher number do not decrease sharply, for instance, even 9th harmonic is lower than the most powerful component ($4f_1$; $4f_2$) or less, than 10 dB (Fig. 23). Noise spectrum in rear hemisphere practically repeats the picture of front hemisphere.

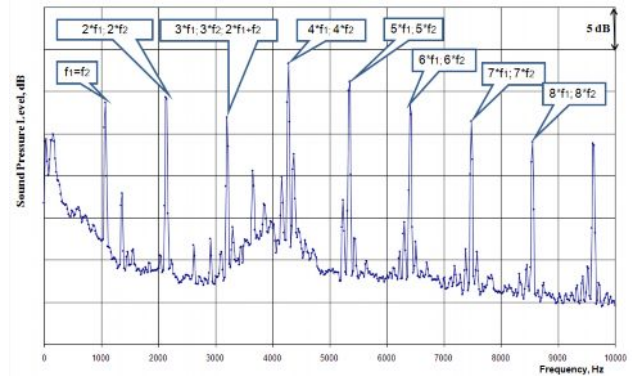


Fig. 23. Narrowband spectra of counter rotating fan model CRTF2b at Flyover mode in direction 60°

On base of CRTF1 and CRTF2b fan model test campaigns, taking into account noise measurement results, comparative computation of noise of hypothetical aircraft with these engines installation was performed in certificated points. Calculations show, that in three certificated points cumulative noise level of aircraft with CRTF2b fan is higher on 10 EPNdB than the aircraft with CRTF1 fan. By all appearances one of the reasons of such result is small value of axial gap between front and aft rotors of CRTF2b model, equal to 0.81, whereas axial gap of CRTF1 model is 1.5 [11].

Conclusions

At CIAM test rig C-3A experimental campaign, investigating acoustic response of three counter-rotating fan models with turbulence control screen (TCS), installed at the inlet and system of air discharging from the anechoic chamber was performed. Tests of fan models were performed within the operating range 40 – 100% from the nominal. CRTF1 fan model was tested with and without acoustic liners installation. In the fan model duct homogeneous liners, developed and manufactured by French company Snecma, was installed. It was discovered, that fan model basic noise was generated by R1 and R2 rotors, counter rotating.

1. It was showed, that counter rotating fan noise spectrum is characterized by availability of the number of tonal components as at BPF and its harmonics at R1, R2 and R3 as combination frequencies including these noise sources interactions. And just tonal components at combination frequencies are the most power carrying ones. Noise spectra of tested counter rotating fan models proved to be unstable, which makes difficult using the experimental campaign results for verification of numerical methods for prediction of ducted counter rotating fan acoustic response.

2. Applied liners significantly reduce fan tonal and broadband noise. Nevertheless, these liners at Approach ensured balanced fan noise radiated in forward and rear hemispheres. At Runway and Flyover noise radiated in rear hemisphere proved to be significantly higher than noise radiated in forward hemisphere at hush kit installed.

3. The C-3A chamber anechoicity in presence of UPS, shafting, a cone and other equipment was verified during preparation to counter rotating fan mockup tests. In [8, 9] it was shown that the anechoic chamber can be used for noise measurements within 200 Hz - 40 kHz.

4. It was shown that CRTF2a counter rotating fan model with thickened blades generates noise, higher than of the CRTF1 model. Comparison of these fans noise spectra at the same modes showed, that broadband noise of fan model with thickened blades was higher than of the model with thin blades on 2...3 dB.

The correlation between tonal noise levels of two fan models is ambiguous. At Runway and Flyover modes in rear hemisphere tonal noise of CRTF1 model is higher than tonal noise of CRTF2a model. Components at frequency, equal to the sum of R1 and R2 BPF, i.e. $(f_1 + f_2)$ dominate in CRTF1 model noise spectrum, while third harmonic of this component dominates in CRTF2a model noise spectrum.

On base of CRTF1 and CRTF2b fan model test campaigns, taking into account noise measurement results, comparative computation of noise of hypothetical aircraft with these engines installation was performed in certificated points. Calculations show, that in three certificated points cumulative noise level of aircraft with CRTF2b fan is higher on 15 EPNdB than the aircraft with CRTF1 fan. By all appearances one of the reasons of such result is small value of axial gap between front and aft rotors of CRTF2b model, equal to 0.81, whereas axial gap of CRTF1 model is 1.5 [9].

References

- [1] Jérôme Talbotec, Michel Vernet. Counter rotating fan aerodynamic design logic & tests results. *Proceeding of the ICAS Conference*, Paper 087, 2010, Nice, France.
- [2] J-M. Cailleau. "CRTF Fan Aerodynamic & Acoustic design & concept Improvement-Preliminary results". Snecma, Budapest Congress & World Trade Centre, 9-10 March, Budapest, Hungary, 2009.
- [3] I. Mileschin, S.V. Pankov, V.A. Fateev "Ducted Counter-Rotating Fan Blades Optimization Based on 3D Inverse Problem Solution aiming at fan gas dynamic improvement". *Proceeding of the ISABE Conference*, ISABE-2009-1334-Paper, Montreal, 2009.
- [4] T. Lengyel, C. Voß, T. Schmidt, E. Nicke. Design of a counter rotating fan. An aircraft engine technology to reduce noise and CO₂-emissions. *Proceeding of the ISABE Conference*, ISABE-2009-1267-Paper Montreal, 2009.
- [5] T. Lengyel- Kampmann, A. Bischoff, R. Meyer, E. Nicke. "Design of an Economical Counter Rotating Fan: Comparison of the Calculated and Measured Steady and Unsteady Results", *Proceedings of the ASME Turbo Expo 2012*, GT2012-69587, 2012, June 11-15, 2012, Copenhagen, Denmark.
- [6] Holste F., Neise W. Experimental determination of the main noise sources in a propfan model by

- analysis of the acoustic spinning modes in the exit plane. *Proc. DGLR/AIAA Aeroacoustics Conference (14th AIAA Aeroacoustics Conference)*, 1992, Aachen, Germany, Paper DGLR/AIAA 92-02-138.
- [7] Holste F., Neise W. Acoustical near field measurement on a propfan model for noise source identification. *Proc. 1st CEAS/AIAA Aeroacoustics Conference (16th AIAA Aeroacoustics Conference)*, 1995, Munich, Germany, Paper CEAS/AIAA-95-178.
- [8] Y. Khaletskiy, R. Shipov, V. Mileschin and V. Povarkov, "New acoustic facility for testing universal propulsion simulators". *Proceeding of the 13th International Congress on Sound and Vibration*, 2006, Vienna, Austria.
- [9] Y. Khaletskiy, V. Mileschin, R. Shipov. Study of counter rotating fan noise at anechoic chamber. *Proceeding of the Conference "EuroNoise"*, 26-28 October, 2009, Edinburgh, Scotland, #0268.
- [10] T. Karimbaev and others. "Light wide chord blades development using composite materials for advanced turbofan", *Modern techniques for providing mechanical reliability of aviation engine parts*, Proceedings of Central Institute of Aviation Motors #1344, Moscow (2010).
- [11] Y. Khaletskiy, R. Shipov, V. Mileschin and V. Povarkov, "Experimental Study of the Counter Rotating Model Fan Noise", *Ecological Problems of Aviation*, Proceedings of Central Institute of Aviation Motors #1347, Moscow (2010), p. 76-83.

Copyright Statement

The authors confirm that they, and/or their company or organization, hold copyright on all of the original material included in this paper. The authors also confirm that they have obtained permission, from the copyright holder of any third party material included in this paper, to publish it as part of their paper. The authors confirm that they give permission, or have obtained permission from the copyright holder of this paper, for the publication and distribution of this paper as part of the ICAS2012 proceedings or as individual off-prints from the proceedings.